CHEMISTRY OF MATERIALS

pubs.acs.org/cm

Article

Origin of Instability of Titanicone Grown by Molecular Layer Deposition Using $TiCl_4$ and Ethylene Glycol

Hyeongjin Kim, Jieun Hyun, Gaeun Kim, Eunsang Lee, and Yo-Sep Min*

Cite This: *Chem. Mater.* 2024, 36, 247−255

Read Online

ACCESS | Metrics & More | Article Recommendations | Supporting Information

ABSTRACT: Titanicone, obtained through molecular layer deposition (MLD) using $TiCl_4$ and ethylene glycol (EG), is often regarded as a thin film of titanium ethylene glycolate [$Ti(OCH_2CH_2O)_2$]. Nevertheless, titanicone exhibits a distinct vulnerability to moisture, while single crystals of $Ti(OCH_2CH_2O)_2$ remain stable, even in the presence of water. To elucidate the origin of instability, we investigated the pathway of chemical degradation for titanicone using in situ and ex situ analytical methods such as Fourier transform infrared spectrometry, quartz crystal microbalance, quadrupole mass spectrometry, and X-ray photoelectron spectroscopy. Our analyses unveiled that the instability of the MLD-grown titanicone film in the presence of water can be primarily attributed to the high chlorine content present as Ti−Cl species and the coexistence of single-reacted EG species as well as double-reacted EG species, unlike in $Ti(OCH_2CH_2O)_2$ crystals. Water molecules react with the Ti−Cl species, leading to the formation of Ti−OH species and the release of HCl gas. Furthermore, the single-reacted EG species undergo an intramolecular cyclization reaction catalyzed by HCl, resulting in the formation of Ti−OH and the liberation of ethylene oxide. Consequently, when exposed to water, the MLD-grown titanicone turns into a water-stable mixed film composed of TiO_2 and $Ti(OCH_2CH_2O)_2$.

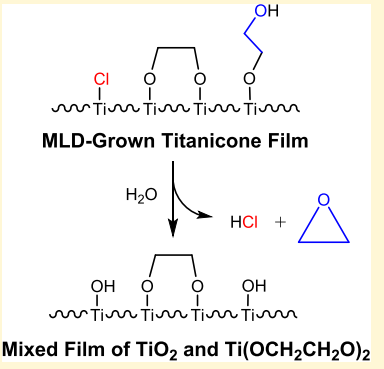

1. INTRODUCTION

Molecular layer deposition (MLD) is a distinct variation of atomic layer deposition (ALD) that enables the production of organic or organic−inorganic hybrid films by adapting multifunctional organic precursors.[1−4] Both MLD and ALD exhibit self-limiting growth behavior, where film growth occurs solely through the chemical adsorption of precursors.[1,5] MLD or a combination of MLD and ALD have been employed for the fabrication of tailored structures of organic or organic−inorganic hybrid films.[4] The unique features of MLD make it a promising method for the fabrication of ultrathin films with tailored properties and functionality.[3,4] For example, MLD has been used to prepare protective coatings for electronic devices,[6] gas permeation barriers,[7] and functional materials for energy storage and conversion.[8] Additionally, MLD has potential applications for drug delivery systems in the biomedical field.[9]

Organic−inorganic hybrid films, called metalcones, are grown by alternating the self-limiting chemisorption of metal precursors and multifunctional organic alcohols.[10,11] Metalcones are classified as a type of metal alkoxides and have several variants such as alucones,[6,12−16] zincones,[17−19] titanicones,[20−23] and hafnicones.[24,25] In general, metalcone films are considered unstable in the air because the moisture present in the air can easily affect the metal−oxygen (M-O) linkages.[6,26] For example, a report by Dameron and colleagues on an alucone, an aluminum ethylene glycolate film prepared by MLD using trimethylaluminum (TMA) and ethylene glycol (EG), showed that the thickness of the alucone film decreased by around 20% after being exposed to air for 200 h.[12] Using in situ Fourier transform infrared spectroscopy (FTIR), they suggested that the film shrinkage was caused by chemical degradation accompanying either dehydration or dehydrogenation of the EG moiety in the alucone.[12] The moisture susceptibility of metalcone films was also observed for zincone and titanicone films grown by MLD using diethylzinc (DEZ) and $TiCl_4$ as metal precursors and EG as bifunctional organic alcohol.[18,20] However, according to a report by Lee et al., a hafnicone film grown using tetrakis(dimethylamido) hafnium (TDMAH) and EG exhibited stability over time in the presence of air.[24] To comprehend the variance in the stability among different metalcones, it is essential to investigate the underlying mechanism of chemical degradation.

On the other hand, the high moisture susceptibility of alucone was rather adapted to transform alucone films into porous alumina by etching the organic components in water.[15] Similarly, it has been reported that titanicone films on silica particles can be converted to titania by decomposing the organic components of the titanicone films in the presence of water.[27] Based on ex situ FTIR analysis, Patel et al. revealed

Received: August 11, 2023
Revised: December 5, 2023
Accepted: December 5, 2023
Published: December 19, 2023

the decomposition of organic components in titanicone films after being exposed to water vapor.[27] However, previous studies on the instability of metalcones have not provided a clear explanation for the decomposition of organic moieties when exposed to water, leading to the formation of porous metal oxide films. The porous films with adjustable thickness could be prepared from metalcone films not only by etching the organic components in water at room temperature but also by calcination at high temperatures.[21,27−30] Several groups have reported the application of this technique in various areas, including electrochemical catalysts, membrane filters, and drug powders.[22,31−33]

Recently, we have reported a mechanistic study on MLD of titanicone from $TiCl_4$ and EG.[23] EG, a type of diol, exhibits a preference for the so-called "double reaction" wherein EG reacts twice with the $TiCl_x$ surface species. However, the resulting surface species, $TiOCH_2CH_2OTi$, formed through the double reaction, can undergo a ring-opening reaction, leading to the regeneration of a single-reacted surface species, $TiOCH_2CH_2OH$. Furthermore, the $TiOCH_2CH_2OH$ surface species can be converted to Ti−OH through an acid-catalyzed intramolecular cyclization. The occurrence of these ring-opening reactions and intramolecular cyclization reactions during the growth of titanicone is attributed to the presence of HCl, which is produced as a byproduct during the chemisorption reactions of $TiCl_4$ and EG. It is suspected that the instability of titanicone grown by MLD using $TiCl_4$ and EG may be related to the evolution of HCl as the titanicone films have a significant amount of Cl content.

To effectively utilize titanicone films in various applications, it is essential to understand the chemical degradation mechanism that occurs when they are exposed to air. This understanding is crucial for improving the stability of titanicone or for preparing porous titanium oxide films by removing the organic components. In this study, we have investigated the underlying causes of the instability of titanicone using in situ and ex situ analytical methods, such as FTIR, quartz crystal microbalance (QCM), quadruple mass spectrometry (QMS), and X-ray photoelectron spectroscopy (XPS).

2. EXPERIMENTAL SECTION

The instability of titanicone films was investigated by monitoring the change in thickness after immersing the titanicone specimens in deionized water. Titanicone films for the water immersion experiment were deposited on boron-doped p-type Si wafers (10 Ω·cm, LG Siltron, Inc.) in a cold-wall reactor (ATOMIC-Classic, CN1 Co., Ltd.) using $TiCl_4$ (99.9%, Sigma-Aldrich) and EG (99.8%, Sigma-Aldrich). Each canister of $TiCl_4$ and EG was kept at room temperature and 60 °C, respectively. Both precursors were led into the reactor without the use of any carrier gas through delivery lines maintained at 100 °C. High-purity nitrogen gas (99.999%) was used as a purging gas with a flow rate of 400 standard cubic centimeters per minute (sccm). The MLD cycle of titanicone consisted of four steps: $TiCl_4$ (1 s)−N_2 purge (5 s)−EG (5 s)−N_2 purge (30 s). The thickness of titanicone films on Si wafers was determined by using a spectroscopic ellipsometer (SE, MG-100, Nano View). The SE had a spectral range of 1.5−5.0 eV and was operated at an incidence angle of around 70°. The measured data were fitted with a dispersion function of the Tauc−Lorentz model for titanicone films. X-ray photoelectron spectra (XPS) were obtained from as-grown and water-immersed titanicone/Si specimens using a PHI 5000 Versaprobe (ULVAC PHI) with monochromatic Al Kα emission. The binding energies were referenced to Au $4f_{7/2}$ at 84.00 eV.

For in situ QCM experiments, we employed a QCM sensor crystal (008−010-G10, Inficon) which was a gold-coated AT-cut quartz crystal with a resonant frequency of 6 MHz.[23,34] The sensor crystal was mounted in a sensor housing attached to the MLD reactor. The change in the frequency of the sensor crystal was measured at 250 ms intervals using an in situ QCM system (WizQCM-1200 Premium, WizMac) during the titanicone MLD or water exposure process. According to the Sauerbrey equation, the change in frequency of the sensor crystal is proportional to the change in mass.[23] A reduction of 1 Hz in frequency corresponds to a mass gain of 6.64 ng/cm^2 in our QCM setup.

To analyze the gaseous species resulting from the chemical degradation of an MLD-grown titanicone film upon exposure to water, an in situ QMS experiment was performed using a residual gas analyzer (Dymaxion, AMETEK, Inc.).[23] Before the QMS experiment, the titanicone film was deposited at 80 °C by repeating sequential MLD steps consisting of $TiCl_4$ exposure (1 s), Ar purging (60 s), EG exposure (5 s), and Ar purging (60 s) for 20 cycles. Subsequently, water vapor was dosed onto the as-grown titanicone for 10 min to monitor the evolution of gaseous species resulting from chemical degradation. A sampling of gaseous species from the MLD reactor to the QMS chamber was accomplished through an orifice of 150 μm. A flexible vacuum bellows served as the delivery line between the reactor and the QMS chamber. To prevent any condensation of the gaseous species, the delivery line was heated to 80 °C. The mass spectrometer was configured with an ionization energy of 70 eV and a dwell time of 3 ms.

For in situ FTIR experiments, an FTIR spectrometer (Nicolet iS50, Thermo Fisher Scientific, Inc.) was installed in the MLD reactor with two opposing ZnSe windows.[23,34,35] The IR beam was aligned in the transmission geometry, passing from the light source through a porous silica pellet, and then detected by a mercury cadmium telluride (MCT) detector. The MCT detector was cooled using liquid nitrogen to achieve high-resolution IR spectra with a resolution of 4 cm^{-1}. All FTIR spectra were obtained by averaging 400 scans. The porous silica pellet was prepared with fumed silica powder (S5505, Sigma-Aldrich) using a stainless-steel grid according to the procedure described elsewhere.[35] For the in situ FTIR experiment, titanicone MLD was performed at 80 °C for 10 cycles with sequential steps of $TiCl_4$ (2 s)−N_2 purge (60 s)−EG (5 s)−N_2 purge (60 s). After the MLD process, the roughing valve between the reactor and the vacuum pump was closed, and then water vapor was supplied into the reactor for several seconds to reach a pressure of about 10 Torr and maintained for a desired time (30 min or 1 h). Subsequently, the reactor was purged with nitrogen gas (400 sccm) for 3 min after the roughing valve.

3. RESULTS AND DISCUSSION

According to a report by Abdulagatov and colleagues, the MLD-grown titanicone film experienced a 20% decrease in thickness over 25 days when exposed to air.[20] Within the first 5 days of air exposure, the thickness decreased by approximately 15% of the initial thickness. We also observed a significant reduction in the thickness of titanicone films over time when kept in the air. Based on the monitoring of thickness variation using SE (Figure 1a), the titanicone film, which was grown at 80 °C using $TiCl_4$ and EG, exhibited a reduction in thickness from 16.0 to 11.8 nm after being exposed to air for 76 h. As moisture present in the air is suspected to cause chemical degradation, which is responsible for the thickness reduction, an in situ QCM analysis was performed as shown in Figure 1b. During the sequential process of titanicone MLD for 10 cycles (black line in Figure 1b), each cycle resulted in an average mass gain of ∼110 ng/cm^2, which is consistent with a previously reported value of ∼109 ng/cm^2.[23] Subsequently, the as-grown titanicone film was subjected to sequential and repetitive exposure to water vapor (10 s) and nitrogen gas (30 s) for 100 cycles (red line in Figure 1b). The cumulative

https://doi.org/10.1021/acs.chemmater.3c02018
Chem. Mater. 2024, 36, 247−255

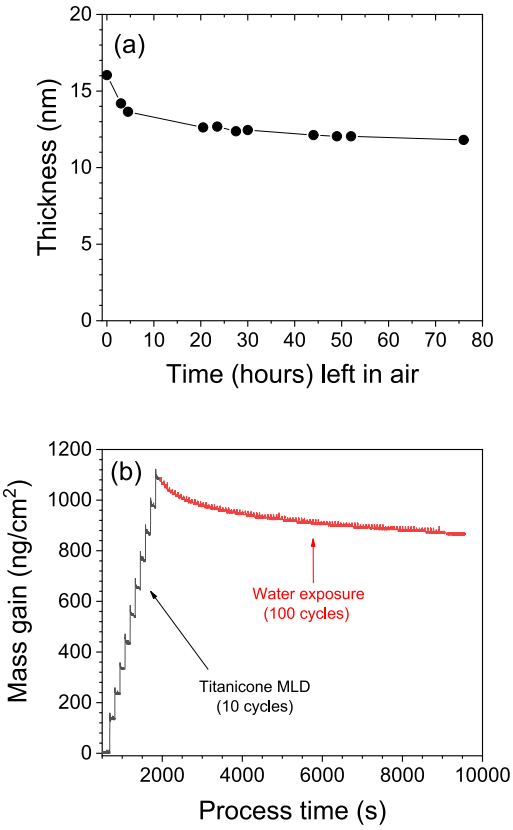

Figure 1. (a) Thickness variation as a function of the time left in the air. The titanicone film grown at 80 °C by MLD [$TiCl_4$ (1 s), purge (5 s), EG (5 s), purge (30 s)] for 50 cycles was left in air at room temperature to monitor its thickness variation using SE. (b) Mass gain as a function of process time. Black and red lines show a mass gain variation at 80 °C during MLD of titanicone for 10 cycles and subsequent water exposure for 100 cycles, respectively. Titanicone MLD: $TiCl_4$ (2 s)−purge (60 s)−EG (5 s)−purge (60 s); water exposure: water (10 s)−purge (60 s).

exposure time to water vapor amounted to 1000 s, and the pressure of the water exposure step was ∼2.3 torr. During the in situ QCM experiment, the mass gain increased to ∼1100 ng/cm^2 by the growth of titanicone film and then decreased to ∼870 ng/cm^2 by the water exposure. In Figure S1, an enlarged version of Figure 1b, under the inert condition achieved through nitrogen purging, there is no mass loss during the latter 30 of the 60 s purging period. In contrast, a significant mass loss is observed upon exposure to water vapor and during the initial 10−20 s of the purging time. The mass loss suggests that the cause of the thickness reduction is moisture present in the air.

To explore the influence of water on the titanicone, titanicone films were deposited onto silicon wafers at 80 °C (50 cycles) and 110 °C (75 cycles). The resulting titanicone/Si specimens were immersed in water, and then the changes in thickness over time during the immersion period were monitored using SE as shown in Figure 2. In the initial 30 s of immersion, the thickness of the titanicone films decreased by half. However, no further changes in thickness were observed during the additional immersion time. Table 1 compares the surface compositions through XPS analyses for both as-grown and water-immersed titanicone films. Note that the compositions of each element were normalized to the titanium content. According to previous studies on the MLD-

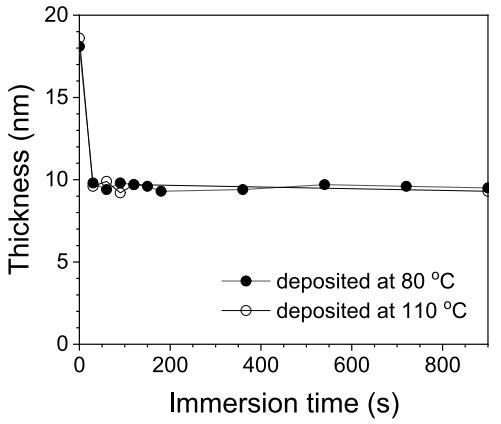

Figure 2. Change in thickness of titanicone according to the time immersed in water at room temperature. The titanicone films were grown at 80 °C (50 cycles) and 110 °C (75 cycles) by using the sequential steps of MLD: $TiCl_4$ (1 s)−purge (5 s)−EG (5 s)−purge (30 s) and their thickness variations were monitored using SE.

grown titanicone,[20,23] it is assumed that the titanicone film grown by MLD using $TiCl_4$ and EG primarily consists of titanium ethylene glycolate [$Ti(OCH_2CH_2O)_2$]. Based on the chemical formula of $Ti(OCH_2CH_2O)_2$, both the theoretical ratios of O/Ti and C/Ti in titanicone are 4:1. The relative contents of oxygen and carbon atoms in the as-grown titanicone film at 110 °C exhibit a stronger similarity to the theoretical value 1:4:4, in comparison to the as-grown film at 80 °C. Furthermore, the as-grown film at 110 °C shows a significantly lower chlorine content (Cl/Ti ∼ 0.49) compared to that of the film grown at 80 °C (∼1.09). These findings can be attributed to the favorable occurrence of the "double reaction", where EG reacts twice with the surface species of $TiCl_x$ at higher temperatures.[23]

After titanicone/Si specimens were immersed in water, there was a significant decrease in the relative contents of oxygen and carbon atoms by chemical degradation during the immersion process. However, it should be noted that the carbon content decreased approximately twice as much as the oxygen content (see the difference values in Table 1). The twice faster rate of decrease of C/Ti compared to that of O/Ti strongly suggests that titanicone undergoes chemical degradation, leading to the liberation of ethylene oxide (OCH_2CH_2) during its water immersion. In addition, the immersion of titanicone in water drastically reduces the Cl content, as the Ti−Cl species can be converted to Ti−OH species by the reaction (eq 1) with water accompanying the release of HCl.

$$Ti - Cl + H_2O \rightarrow Ti - OH + HCl \quad (1)$$

Figure 3 compares the XPS spectra of titanicone/Si specimens (grown at 110 °C) before and after immersion in water (refer to Figure S2 for a similar comparison of XPS spectra of specimens grown at 80 °C). Notable changes in the peak positions of the binding energy are observed, particularly in the O 1s and the C 1s core electrons. Additionally, the doublet of Cl 2p nearly disappears after immersion in water. Nevertheless, considering that the as-grown specimen was exposed to air before the XPS analysis, there is a concern that a detailed interpretation of the spectra (red line) from the as-grown specimen may lead to excessive conclusions given that the as-grown titanicone film has already deteriorated.

https://doi.org/10.1021/acs.chemmater.3c02018
Chem. Mater. 2024, 36, 247−255

Table 1. Relative Surface Compositions based on XPS Analyses of Titanicone Grown at 80 and 110 °C: Comparison of As-Grown and Water-Immersed Titanicone Films[a]

	MLD-grown titanicone at 80 °C			MLD-grown titanicone at 110 °C		
elements	as-grown	immersed	difference	as-grown	immersed	difference
Ti	1.00	1.00		1.00	1.00	
O	3.63	2.53	1.10	3.77	3.02	0.75
C	4.53	2.10	2.43	3.86	2.02	1.84
Cl	1.09			0.49	0.07	

[a]The relative surface compositions were determined by normalizing the contents of each element to that of the Ti atom.

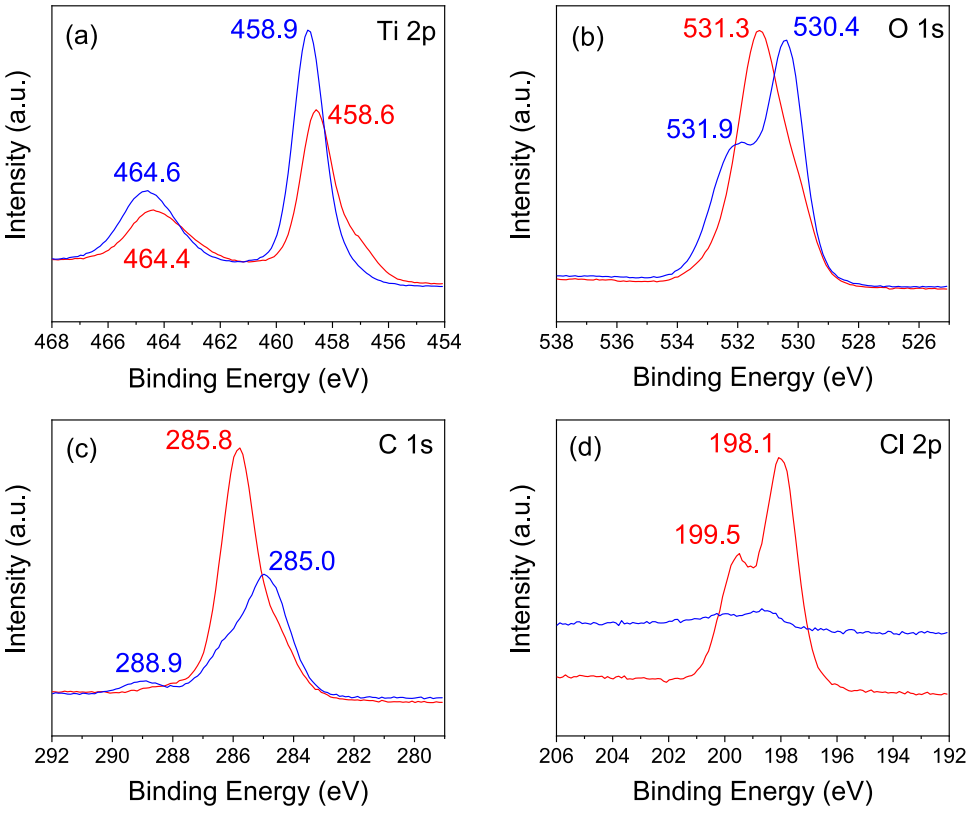

Figure 3. XPS spectra of (a) Ti 2p, (b) O 1s, (c) C 1s, and (d) Cl 2p core electrons of as-grown (at 110 °C, red line) and water-immersed (blue line) titanicone/Si specimens.

However, analysis of XPS spectra (blue line in Figure 3) obtained from the water-immersed titanicone film provides valuable insights into the chemical degradation that occurs when the film is exposed to water. In Figure 3a, the characteristic binding energies of Ti $2p_{1/2}$ and $2p_{3/2}$, which are attributed to Ti^{4+}, were observed at 464.6 and 458.9 eV, respectively.[36] Remarkably, the binding energy of the O 1s core electrons (Figure 3b) appeared at 530.4 eV, accompanied by a shoulder at 531.9 eV. This observation suggests the existence of two distinct types of oxygen atoms exhibiting different chemical states. The broad and asymmetric peak of C 1s in Figure 3c was observed at 285.0 eV, which is mainly attributed to adventitious carbon since the XPS spectra were obtained from the virgin surface where adventitious carbon was not removed. Nevertheless, a shoulder at approximately 286 eV indicates the presence of carbon atoms bonded to oxygen (C–O).[37] In addition, the doublet peaks of Cl 2p core electrons are very weak due to the removal of chlorine through its reaction with water (eq 1).

As previously mentioned, the as-grown titanicone is believed to be a thin film primarily composed of titanium ethylene glycolate [$Ti(OCH_2CH_2O)_2$].[20,23] Wang and co-workers elucidated the crystal structure of titanium ethylene glycolate prepared by a solvothermal synthesis method.[38] The needle-like single crystal of titanium ethylene glycolate exhibits a *C*-centered monoclinic structure belonging to the space group *C*2/*c*. The crystal consists of one-dimensional chains formed by $Ti^{4+}O_6$ octahedra sharing edges along the *c*-axis. Consequently, every EG molecule undergoes a double reaction, leading to the formation of ethylene glycolate ($-OCH_2CH_2O-$) and resulting in the presence of two terminal oxygen atoms and four bridging oxygen atoms within the $Ti^{4+}O_6$ octahedra. It should be noted that the single crystal was analyzed after washing with water since it was stable in water, unlike the as-grown titanicone film by MLD.[38,39]

Han and colleagues reported XPS spectra of the crystal of $Ti(OCH_2CH_2O)_2$ prepared by a solvothermal method.[39] Table 2 provides a comparison of the binding energies of core electrons between the water-immersed titanicone and the crystalline $Ti(OCH_2CH_2O)_2$. Comparing the binding energies of O 1s core electrons in two distinct chemical states of titanicone with that of O 1s in $Ti(OCH_2CH_2O)_2$, the presence

https://doi.org/10.1021/acs.chemmater.3c02018
Chem. Mater. 2024, 36, 247−255

Table 2. Binding Energies of Core Electrons in Water-Immersed Titanicone by XPS

	binding energy (eV)	
core electron	titanicone[a]	crystalline $Ti(OCH_2CH_2O)_2$[b]
Ti $2p_{1/2}$	464.6	464.6
Ti $2p_{3/2}$	458.9	458.9
O 1s (oxide)	530.4	
O 1s (glycolate)	531.9[c]	~531.7
C 1s (adventitious)	285.0	285.2[c]
C 1s (glycolate)	~286[c]	286.2

[a]Grown at 110 °C and then immersed in water for 30 s. [b]Han et al. (ref 39). [c]These peaks were observed as a shoulder of a main peak.

of a shoulder at 531.9 eV in the O 1s spectrum (Figure 3b) of the water-immersed titanicone film is attributed to the oxygen atoms in the ethylene glycolate moiety. On the other hand, the other O 1s peak at 530.4 eV is assigned to TiO_2, which is formed through the chemical degradation of titanicone upon exposure to water. In Figure S3d, the O1s spectrum of the water-immersed specimen was deconvoluted into two peaks at 532.1 eV (glycolate) and 530.4 eV (TiO_2), respectively. Furthermore, the presence of a shoulder in the C 1s peak at ~286 eV in Figure 3c (deconvoluted at 286.4 eV in Figure S3f) aligns well with the C 1s peak observed at 286.2 eV in $Ti(OCH_2CH_2O)_2$. This suggests that the water-immersed titanicone film remains stable in water (Figure 2) since it is composed of a combination of TiO_2 and $Ti(OCH_2CH_2O)_2$, forming a mixed film.

Based on recent XPS studies on Ti-containing oxides, researchers have found a correlation between the chemical state of Ti and the binding energy difference Δ(O−Ti) between O 1s and Ti $2p_{3/2}$.[36] This correlation is visually presented in Figure 4 (open circles), where data from ref 36

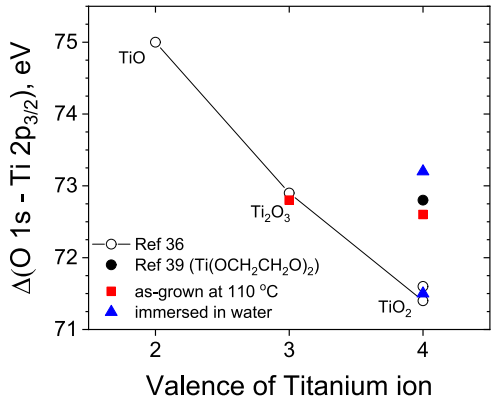

Figure 4. Binding energy difference between O 1s and Ti $2p_{3/2}$ as a function of the valence of the titanium ion. The data values of the as-grown (red squares) and immersed (blue triangles) titanicone specimens were obtained from the deconvoluted spectra shown in Figure S3.

are plotted. The Δ(O−Ti) value decreases with the valence of titanium ion, starting from 75.0 eV for TiO (divalent) through 72.9 eV for Ti_2O_3 (trivalent), and reaching approximately 71.5 eV for TiO_2 (tetravalent). They found that the observed decreasing trend in the Δ(O−Ti) value is due to the shorter bond length of Ti−O in oxides of which the titanium ion has a higher valence. Based on the XPS data in Table 2 (ref 39), the Δ(O−Ti) value of crystalline $Ti(OCH_2CH_2O)_2$ is approximately 72.8 eV (solid circle in Figure 4), even though the titanium ethylene glycolate crystal consists of tetravalent titanium ions and ethylene glycolate ligands. In the crystallographic structure of $Ti(OCH_2CH_2O)_2$, the $Ti^{4+}O_6$ octahedra consist of two terminal and four bridging oxygen atoms.[38] Furthermore, the average Ti−O length of the bridging oxygen atoms is approximately 17 pm longer (~200.4 pm) compared with the Ti−O length of the terminal oxygen atoms (~183.7 pm). This elongation of Ti−O length in the bridging oxygen atoms is believed to be the underlying reason for the unusual increase in the Δ(O−Ti) value observed in the crystal of $Ti(OCH_2CH_2O)_2$. As mentioned above, since the water-immersed titanicone is a mixed film mainly composed of TiO_2 and $Ti(OCH_2CH_2O)_2$, the two Δ(O−Ti) values (71.5 and 73.2 eV) of the titanicone are plotted close to those of TiO_2 and crystalline $Ti(OCH_2CH_2O)_2$, respectively, as represented by triangles in Figure 4.

Based on the comparison of deconvoluted XPS spectra in Figures S3 (titanicone grown at 110 °C) and S4 (at 80 °C) for as-grown and water-immersed titanicone/Si specimens, the shoulder of the O 1s peak in the as-grown specimen is not clear and deconvoluted at significantly different positions from the water-immersed specimen. Considering the Δ(O−Ti) values from the deconvoluted spectra of the so-called as-grown specimen, which has already deteriorated in air, the as-grown titanicone contains a small portion of titanium suboxide such as Ti_2O_3, with the Ti^{3+} $2p_{3/2}$ and O 1s peaks deconvoluted at 457.2 and 530.0 eV, respectively (as indicated by red squares in Figure 4).

In Scheme 1, we present a plausible mechanism for the chemical degradation of MLD-grown titanicone. The as-grown titanicone film (I) contains not only $-OCH_2CH_2O-$ species resulting from the double reaction of EG but also $-OCH_2CH_2OH$ species from the single reaction of EG. Furthermore, there are a considerable number of chlorine atoms in the as-grown film, which was confirmed by XPS analysis. When the MLD-grown titanicone film is exposed to water, the Ti−Cl species undergo a hydroxylation reaction (from I to II), liberating hydrogen chloride gas. The liberated HCl can then act as an acid catalyst for an intramolecular cyclization reaction, as previously reported.[23] This reaction leads to the formation of Ti−OH species and the release of gaseous ethylene oxide (from II through III to IV in Scheme 1).

Based on the proposed mechanism, the chemical degradation of the MLD-grown titanicone film caused by water exposure is expected to result in the liberation of gaseous hydrogen chloride (HCl) and ethylene oxide (CH_2CH_2O). To validate this degradation pathway, we conducted an in situ QMS experiment. Following the deposition of titanicone for 20 MLD cycles (as detailed in the Section 2), water vapor (m/z = 18) was introduced onto the as-grown titanicone film. During this process, the expected gaseous species, hydrogen chloride (m/z = 36) and ethylene oxide (m/z = 44), were clearly observed, as shown in Figure 5. The detection of these two compounds provides strong evidence supporting the validity of the proposed mechanism. During the chemical degradation of as-grown titanicone films, the release of ethylene oxide leads to a decrease in both carbon and oxygen contents. Considering the chemical formula of ethylene oxide (CH_2CH_2O), the expected relative decrease rate for carbon and oxygen is 2:1. Remarkably, the decrease in carbon and oxygen contents observable by XPS (Table 1) aligns closely with this theoretical

https://doi.org/10.1021/acs.chemmater.3c02018
Chem. Mater. 2024, 36, 247−255

Scheme 1. Plausible Mechanism for Chemical Degradation of MLD-Grown Titanicone Film

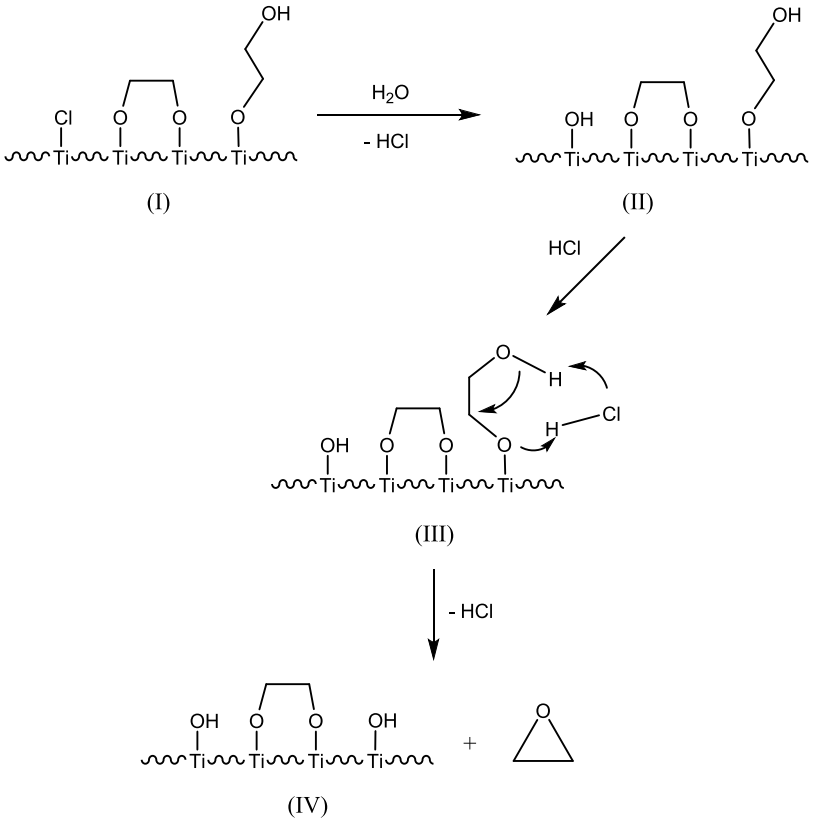

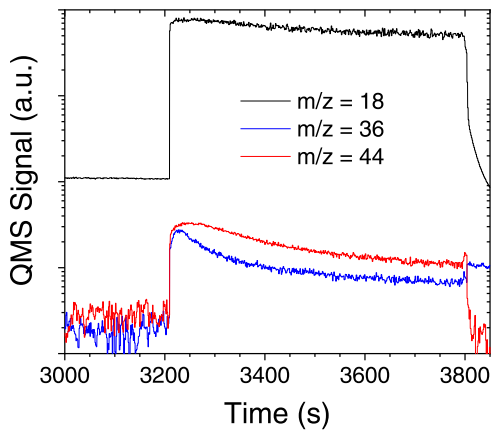

Figure 5. In situ QMS signal traces of fragments m/z = 18 (H_2O^+), 36 (HCl^+), and 44 ($CH_2CH_2O^+$) when an MLD-grown titanicone film was exposed to water vapor for 10 min.

value. In Figure 2, despite the significantly different ratios of Cl/Ti between two as-grown titanicone specimens (1.09 for the 80 °C-grown and 0.49 for the 110 °C-grown titanicone), the thickness reductions after the water immersion are similar to each other. If the Cl content exceeds the amount of the single-reacted OCH_2CH_2OH species, then the excess quantity of Cl beyond the amount of the single-reacted EG species may not contribute to the thickness reduction.

Using an in situ FTIR spectrometer, the changes in the ethylene moiety within a titanicone film upon exposure to water vapor can be analyzed with "difference spectra". A difference spectrum obtained in a specific step, termed Step A, is referenced to the spectrum acquired in a designated preceding step, termed Step B, during the in situ FTIR experiment. As a result, positive and negative vibrational peaks in the difference spectrum (Step A minus Step B) indicate the presence of surface species that have been produced and consumed, respectively, between Step A and Step B.

In Figure 6a, the black difference spectrum was obtained from an as-grown titanicone film (10 MLD cycles) and referenced to a bare silica pellet. The observed sharp negative peak at 3747 cm^{-1} and its broad negative shoulder at around 3500 cm^{-1} indicate that isolated and hydrogen-bonded hydroxyl groups on the bare silica surface have been consumed during the process of MLD cycles repeated 10 times for the growth of the titanicone film. Furthermore, the appearance of two positive peaks at 2935 and 2874 cm^{-1}, which are assigned to the antisymmetric ν_{as}(C−H) and symmetric ν_s(C−H) stretching vibrations of the ethylene moiety, indicates the incorporation of the ethylene moiety into the titanicone film during the MLD process.

The red difference spectrum in Figure 6a was acquired by exposing the 10 MLD-cycled titanicone to water vapor for 30 min. Therefore, this difference spectrum represents the changes in chemical species that occurred in the as-grown titanicone during the 30 min water exposure. The presence of a positive sharp peak at 3745 cm^{-1} indicates the formation of isolated hydroxyl groups. These hydroxyl groups are likely produced through the pathway described in Scheme 1. However, the appearance of positive peaks at 2935 and 2863 cm^{-1} for the stretching bands of ν_{as}(C−H) and ν_s(C−H), respectively, contradicts the expectation of negative vibrational bands associated with the liberation of ethylene oxide. Furthermore, there is no significant peak in the blue spectrum

https://doi.org/10.1021/acs.chemmater.3c02018
Chem. Mater. 2024, 36, 247−255

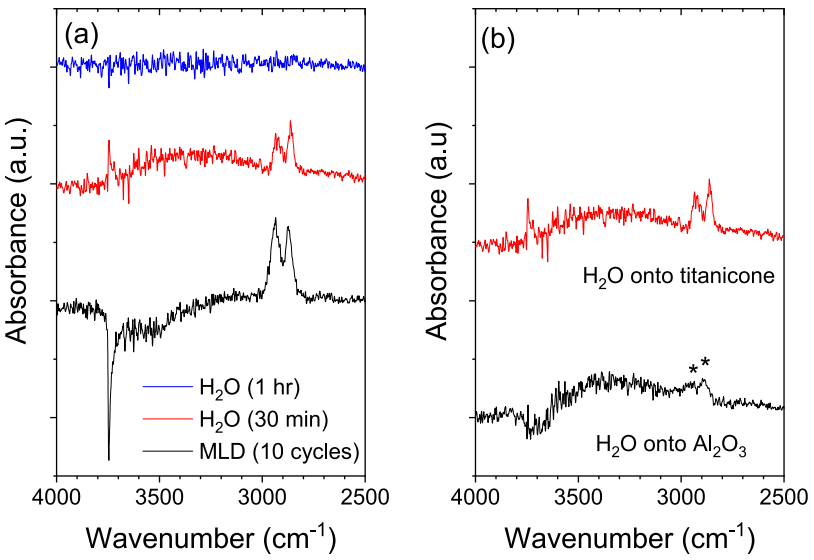

Figure 6. (a) In situ FTIR difference spectra of as-grown titanicone for 10 MLD cycles (black), water-exposed titanicone for 30 min (red), and water-exposed titanicone for an additional one hour (blue). (b) In situ FTIR difference spectra of water-exposed titanicone for 30 min (red) and water-exposed Al_2O_3 for 30 min (black).

of Figure 6a, which was obtained by an additional 1 h water exposure to the 10 MLD-cycled titanicone.

It is worth noting that the reaction from II to IV in Scheme 1 can reverse if there is an excess supply of ethylene oxide to the titanicone film compared to the amount removed from the film. During the MLD process, the growth of titanicone films occurs not only on the surface of the silica pellet (where the spectrum was obtained) but also on the entire wall of the MLD reactor. We attribute the positive C−H stretching vibrations in the red spectrum (Figure 6a) to the readsorption of liberated ethylene oxide from the titanicone films grown on the reactor wall. The readsorption of ethylene oxide onto the titanicone film may be catalyzed by HCl, which is released by the reaction between the Ti−Cl species and water. The absence of C−H stretching peaks in the blue spectrum (Figure 6a) after an additional 1 h exposure to water vapor can indeed be explained by considering the assumption of readsorption. Due to the depletion of ethylene oxide during the first 30 min exposure to water vapor, there was an insufficient amount of ethylene oxide available to readsorb onto the surface during the additional 1 h exposure.

To validate the readsorption of ethylene oxide, we conducted a 20-cycle MLD process to grow titanicone on the entire wall of the MLD reactor. In parallel, we performed 10 cycles of Al_2O_3 ALD on a bare silica pellet at 80 °C using TMA and water in a separate ALD reactor.[35] The sequential steps for Al_2O_3 ALD were TMA (1 s)−N_2 purge (10 s)−H_2O (1 s)−N_2 purge (10 s). Then, the Al_2O_3-deposited silica pellet was carefully transferred from the ALD reactor to the MLD reactor. Subsequently, the Al_2O_3-coated silica pellet was exposed to water vapor for 30 min. Figure 6b presents a comparison of the difference spectra of the titanicone (red) and the Al_2O_3 (black) films after the 30 min exposure to water vapor. Remarkably, the C−H stretching bands are observed in the black spectrum of Al_2O_3 (indicated by asterisks), similar to their presence in the red spectrum of the titanicone film. This observation provides strong support for the readsorption of ethylene oxide, which is liberated from the reactor wall when water vapor is supplied to the reactor.

Building upon our proposed mechanism, the chemical degradation involving dehydrogenation and/or dehydration, as suggested for the thickness reduction of as-grown alucone in air, may also contribute to the degradation of titanicone.[6,12,26] The C 1s spectra of water-immersed titanicone specimens in Figures 3c and S2c are deconvoluted into three types of carbons: ethylene glycolate, adventitious carbon, and C═O (refer to Figures S3f and S4f). Although the peak intensity of carbon at ∼289 eV is weak, it is assigned to the C 1s of C═O, and a similar peak was also observed at ∼289 eV in alucone left in the air for several days.[12] The dehydrogenation of the $HOCH_2CH_2OTi$ species could lead to an enol species of $HOCH{=}CHOTi$ and H_2. Subsequently, the enol species may undergo rearrangement to form a keto species of $O{=}CHCH_2OTi$. It has been previously reported that TiO_2 catalyzes the dehydrogenation of adsorbed aliphatic alcohols including EG.[40,41]

4. CONCLUSIONS

While MLD-grown titanicone is often recognized as a thin film of titanium ethylene glycolate, it exhibits a distinct vulnerability to moisture compared to stable titanium ethylene glycolate. Through a comprehensive investigation employing in situ FTIR, QCM, and QMS experiments, in addition to ex situ XPS analysis, the instability of titanicone films, grown by MLD from $TiCl_4$ and EG, was explored to determine the pathway of chemical degradation of titanicone when exposed to water. The instability of titanicone in the presence of water is due to the high chlorine content (i.e., Ti−Cl species) and the coexistence of single-reacted EG species with double-reacted EG species. Water molecules react with the Ti−Cl species, leading to the formation of Ti−OH species and the release of HCl gas. Additionally, the single-reacted EG species undergo an intramolecular cyclization reaction, catalyzed by HCl, resulting in the formation of Ti−OH and the release of ethylene oxide. As a result, the MLD-grown titanicone film transforms into a water-stable mixed film, comprising TiO_2 and $Ti(OCH_2CH_2O)_2$, when exposed to water.

https://doi.org/10.1021/acs.chemmater.3c02018
Chem. Mater. 2024, 36, 247−255

■ ASSOCIATED CONTENT

Supporting Information

The Supporting Information is available free of charge at https://pubs.acs.org/doi/10.1021/acs.chemmater.3c02018.

Magnified QCM data of Figure 1b; XPS spectra of as-grown (80 °C) and water-immersed titanicone/Si; and deconvoluted XPS spectra (PDF)

■ AUTHOR INFORMATION

Corresponding Author

Yo-Sep Min − *Department of Chemical Engineering, Konkuk University, Seoul 05029, Korea;* orcid.org/0000-0002-2340-3633; Email: ysmin@konkuk.ac.kr

Authors

Hyeongjin Kim − *Department of Chemical Engineering, Konkuk University, Seoul 05029, Korea*

Jieun Hyun − *Department of Chemical Engineering, Konkuk University, Seoul 05029, Korea*

Gaeun Kim − *Department of Chemical Engineering, Konkuk University, Seoul 05029, Korea*

Eunsang Lee − *Department of Chemical Engineering, Konkuk University, Seoul 05029, Korea*

Complete contact information is available at: https://pubs.acs.org/10.1021/acs.chemmater.3c02018

Notes

The authors declare no competing financial interest.

■ ACKNOWLEDGMENTS

This work was supported by Konkuk University in 2019.

■ REFERENCES

(1) George, S. M.; Yoon, B.; Dameron, A. A. Surface Chemistry for Molecular Layer Deposition of Organic and Hybrid Organic−Inorganic Polymers. *Acc. Chem. Res.* **2009**, *42* (4), 498−508.

(2) Sundberg, P.; Karppinen, M. Organic and inorganic-organic thin film structures by molecular layer deposition: A review. *Beilstein J. Nanotechnol.* **2014**, *5*, 1104−1136.

(3) Meng, X. An overview of molecular layer deposition for organic and organic−inorganic hybrid materials: mechanisms, growth characteristics, and promising applications. *J. Mater. Chem. A* **2017**, *5* (35), 18326−18378.

(4) Multia, J.; Karppinen, M. Atomic/Molecular Layer Deposition for Designer's Functional Metal−Organic Materials. *Adv. Mater. Interfaces* **2022**, *9* (15), No. 2200210, DOI: 10.1002/admi.202200210.

(5) George, S. M. Atomic Layer Deposition: An Overview. *Chem. Rev.* **2010**, *110* (1), 111−131.

(6) Choi, D.-w.; Yoo, M.; Lee, H. M.; Park, J.; Kim, H. Y.; Park, J.-S. A Study on the Growth Behavior and Stability of Molecular Layer Deposited Alucone Films Using Diethylene Glycol and Trimethyl Aluminum Precursors, and the Enhancement of Diffusion Barrier Properties by Atomic Layer Deposited Al2O3 Capping. *ACS Appl. Mater. Interfaces* **2016**, *8* (19), 12263−12271.

(7) Tseng, M.-H.; Su, D.-Y.; Chen, G.-L.; Tsai, F.-Y. Nano-Laminated Metal Oxides/Polyamide Stretchable Moisture- and Gas-Barrier Films by Integrated Atomic/Molecular Layer Deposition. *ACS Appl. Mater. Interfaces* **2021**, *13* (23), 27392−27399.

(8) Zhao, Y.; Zhang, L.; Liu, J.; Adair, K.; Zhao, F.; Sun, Y.; Wu, T.; Bi, X.; Amine, K.; Lu, J.; et al. Atomic/molecular layer deposition for energy storage and conversion. *Chem. Soc. Rev.* **2021**, *50* (6), 3889−3956. 10.1039/D0CS00156B

(9) Zhang, F.; Wu, K.; La Zara, D.; Sun, F.; Quayle, M. J.; Petersson, G.; Folestad, S.; Chew, J. W.; van Ommen, J. R. Tailoring the flow properties of inhaled micronized drug powders by atomic and molecular layer deposition. *Chem. Eng. J.* **2023**, *462*, No. 142131.

(10) George, S. M.; Lee, B. H.; Yoon, B.; Abdulagatov, A. I.; Hall, R. A. Metalcones: hybrid organic-inorganic films fabricated using atomic and molecular layer deposition techniques. *J. Nanosci. Nanotechnol.* **2011**, *11* (9), 7948−7955.

(11) Lee, B. H.; Yoon, B.; Abdulagatov, A. I.; Hall, R. A.; George, S. M. Growth and Properties of Hybrid Organic-Inorganic Metalcone Films Using Molecular Layer Deposition Techniques. *Adv. Funct. Mater.* **2013**, *23* (5), 532−546.

(12) Dameron, A. A.; Seghete, D.; Burton, B. B.; Davidson, S. D.; Cavanagh, A. S.; Bertrand, J. A.; George, S. M. Molecular Layer Deposition of Alucone Polymer Films Using Trimethylaluminum and Ethylene Glycol. *Chem. Mater.* **2008**, *20* (10), 3315−3326.

(13) Seghete, D.; Davidson, B. D.; Hall, R. A.; Chang, Y. J.; Bright, V. M.; George, S. M. Sacrificial layers for air gaps in NEMS using alucone molecular layer deposition. *Sens. Actuators, A* **2009**, *155* (1), 8−15.

(14) DuMont, J. W.; George, S. M. Pyrolysis of Alucone Molecular Layer Deposition Films Studied Using In Situ Transmission Fourier Transform Infrared Spectroscopy. *J. Phys. Chem. C* **2015**, *119* (26), 14603−14612.

(15) Van de Kerckhove, K.; Barr, M. K. S.; Santinacci, L.; Vereecken, P. M.; Dendooven, J.; Detavernier, C. The transformation behaviour of "alucones", deposited by molecular layer deposition, in nanoporous Al2O3 layers. *Dalton Trans.* **2018**, *47* (16), 5860−5870.

(16) Park, Y.-S.; Kim, H.; Cho, B.; Lee, C.; Choi, S.-E.; Sung, M. M.; Lee, J. S. Intramolecular and Intermolecular Interactions in Hybrid Organic−Inorganic Alucone Films Grown by Molecular Layer Deposition. *ACS Appl. Mater. Interfaces* **2016**, *8* (27), 17489−17498.

(17) Elam, J. W.; George, S. M. Growth of ZnO/Al2O3 Alloy Films Using Atomic Layer Deposition Techniques. *Chem. Mater.* **2003**, *15* (4), 1020−1028.

(18) Yoon, B.; O'Patchen, J. L.; Seghete, D.; Cavanagh, A. S.; George, S. M. Molecular Layer Deposition of Hybrid Organic-Inorganic Polymer Films using Diethylzinc and Ethylene Glycol. *Chem. Vap. Deposition* **2009**, *15* (4−6), 112−121.

(19) Peng, Q.; Gong, B.; VanGundy, R. M.; Parsons, G. N. "Zincone" Zinc Oxide−Organic Hybrid Polymer Thin Films Formed by Molecular Layer Deposition. *Chem. Mater.* **2009**, *21* (5), 820−830.

(20) Abdulagatov, A. I.; Hall, R. A.; Sutherland, J. L.; Lee, B. H.; Cavanagh, A. S.; George, S. M. Molecular Layer Deposition of Titanicone Films using TiCl4 and Ethylene Glycol or Glycerol: Growth and Properties. *Chem. Mater.* **2012**, *24* (15), 2854−2863.

(21) Abdulagatov, A. I.; Terauds, K. E.; Travis, J. J.; Cavanagh, A. S.; Raj, R.; George, S. M. Pyrolysis of Titanicone Molecular Layer Deposition Films as Precursors for Conducting TiO2/Carbon Composite Films. *J. Phys. Chem. C* **2013**, *117* (34), 17442−17450.

(22) Ishchuk, S.; Taffa, D. H.; Hazut, O.; Kaynan, N.; Yerushalmi, R. Transformation of Organic−Inorganic Hybrid Films Obtained by Molecular Layer Deposition to Photocatalytic Layers with Enhanced Activity. *ACS Nano* **2012**, *6* (8), 7263−7269.

(23) Kim, H.; Hyun, J.; Min, Y.-S. Mechanistic Study on Molecular Layer Deposition of Titanicone from TiCl4 and Ethylene Glycol. *J. Phys. Chem. C* **2023**, *127* (5), 2258−2265.

(24) Lee, B. H.; Anderson, V. R.; George, S. M. Growth and Properties of Hafnicone and HfO2/Hafnicone Nanolaminate and Alloy Films Using Molecular Layer Deposition Techniques. *ACS Appl. Mater. Interfaces* **2014**, *6* (19), 16880−16887.

(25) Shi, J.; Ravi, A.; Richey, N. E.; Gong, H.; Bent, S. F. Molecular Layer Deposition of a Hafnium-Based Hybrid Thin Film as an Electron Beam Resist. *ACS Appl. Mater. Interfaces* **2022**, *14* (23), 27140−27148.

(26) Ghazaryan, L.; Kley, E.-B.; Tünnermann, A.; Viorica Szeghalmi, A. Stability and annealing of alucones and alucone alloys. *J. Vac. Sci. Technol., A* **2012**, *31* (1), No. 01A149, DOI: 10.1116/1.4773296.

(27) Patel, R. L.; Jiang, Y.-B.; Liang, X. Highly porous titania films coated on sub-micron particles with tunable thickness by molecular

layer deposition in a fluidized bed reactor. *Ceram. Int.* **2015**, *41* (2, Part A), 2240−2246, DOI: 10.1016/J.CERAMINT.2014.10.026.
(28) Liang, X.; Yu, M.; Li, J.; Jiang, Y. B.; Weimer, A. W. Ultra-thin microporous-mesoporous metal oxide films prepared by molecular layer deposition (MLD). *Chem. Commun.* **2009**, No. 46, 7140−7142.
(29) Liang, X.; Weimer, A. W. An overview of highly porous oxide films with tunable thickness prepared by molecular layer deposition. *Curr. Opin. Solid State Mater. Sci.* **2015**, *19* (2), 115−125.
(30) Perrotta, A.; Poodt, P.; van den Bruele, F. J. F.; Kessels, W.; Creatore, M. Characterization of nano-porosity in molecular layer deposited films. *Dalton Trans.* **2018**, *47* (23), 7649−7655.
(31) Chen, H.; Jia, X.; Wei, M.; Wang, Y. Ceramic tubular nanofiltration membranes with tunable performances by atomic layer deposition and calcination. *J. Membr. Sci.* **2017**, *528*, 95−102.
(32) Wu, S.; Wang, Z.; Xiong, S.; Wang, Y. Tailoring TiO2 membranes for nanofiltration and tight ultrafiltration by leveraging molecular layer deposition and crystallization. *J. Membr. Sci.* **2019**, *578*, 149−155.
(33) Zara, D. L.; Zhang, F.; Sun, F.; Bailey, M. R.; Quayle, M. J.; Petersson, G.; Folestad, S.; van Ommen, J. R. Drug powders with tunable wettability by atomic and molecular layer deposition: From highly hydrophilic to superhydrophobic. *Appl. Mater. Today* **2021**, *22*, No. 100945, DOI: 10.1016/j.apmt.2021.100945.
(34) Hyun, J.; Kim, H.; Shong, B.; Min, Y.-S. Pyridine-Catalyzed Atomic Layer Deposition of SiO2 from Hexachlorodisilane and Water: An In Situ Mechanistic Study. *Chem. Mater.* **2023**, *35* (10), 4100−4108.
(35) Jin, Z.; Lee, S.; Shin, S.; Shin, D.-S.; Choi, H.; Min, Y.-S. Chemical Probing of Water-Stable Methyl Species in Atomic Layer Deposition of Al2O3 from Trimethylaluminum and Water. *J. Phys. Chem. C* **2021**, *125* (39), 21434−21442.
(36) Atuchin, V. V.; Kesler, V. G.; Pervukhina, N. V.; Zhang, Z. Ti 2p and O 1s core levels and chemical bonding in titanium-bearing oxides. *J. Electron Spectrosc. Relat. Phenom.* **2006**, *152* (1), 18−24.
(37) Chen, X.; Wang, X.; Fang, D. A review on C1s XPS-spectra for some kinds of carbon materials. *Fullerenes, Nanotubes Carbon Nanostruct.* **2020**, *28* (12), 1048−1058.
(38) Wang, D.; Yu, R.; Kumada, N.; Kinomura, N. Hydrothermal Synthesis and Characterization of a Novel One-Dimensional Titanium Glycolate Complex Single Crystal: Ti(OCH2CH2O)2. *Chem. Mater.* **1999**, *11* (8), 2008−2012.
(39) Han, W.; Yang, X.; Zhao, F.; Shi, X.; Wang, T.; Zhang, X.; Jiang, L.; Wang, C. A mesoporous titanium glycolate with exceptional adsorption capacity to remove multiple heavy metal ions in water. *RSC Adv.* **2017**, *7* (48), 30199−30204.
(40) Farfan-Arribas, E.; Madix, R. J. Role of Defects in the Adsorption of Aliphatic Alcohols on the TiO2(110) Surface. *J. Phys. Chem. B* **2002**, *106* (41), 10680−10692.
(41) Li, Z.; Kay, B. D.; Dohnálek, Z. Dehydration and dehydrogenation of ethylene glycol on rutile TiO2(110). *Phys. Chem. Chem. Phys.* **2013**, *15* (29), 12180−12186.

https://doi.org/10.1021/acs.chemmater.3c02018
Chem. Mater. 2024, 36, 247−255

Supporting Information

Origin of Instability of Titanicone Grown by Molecular Layer Deposition Using $TiCl_4$ and Ethylene Glycol

Hyeongjin Kim, Jieun Hyun, Gaeun Kim, Eunsang Lee, and Yo-Sep Min*

Department of Chemical Engineering, Konkuk University, 120 Neungdong-Ro, Gwangjin-Gu, Seoul 05029, Korea

*Y. S. Min. Email: ysmin@konkuk.ac.kr

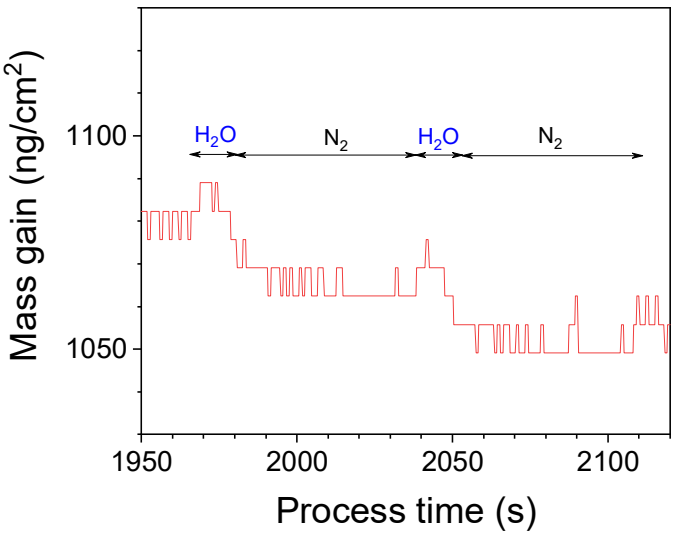

Figure S1. Magnified data of mass gain as a function of process time in Figure 1b: water exposure (10 s) and nitrogen gas purging (60 s).

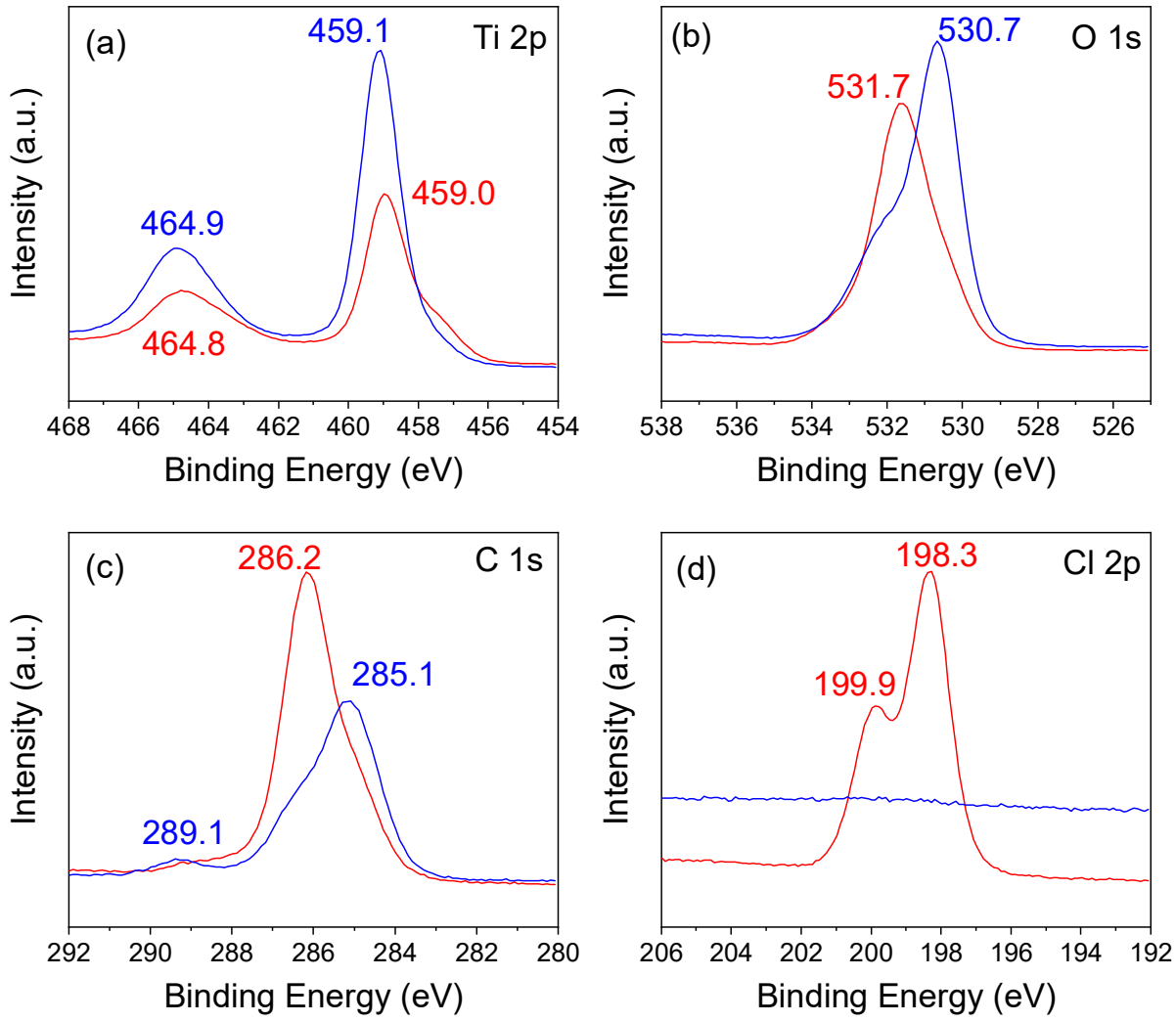

Figure S2. XPS spectra of (a) Ti 2p, (b) O 1s, (c) C 1s, and (d) Cl 2p core electrons of as-grown (at 80 ℃, red line) and water-immersed (blue line) titanicone/Si specimens.

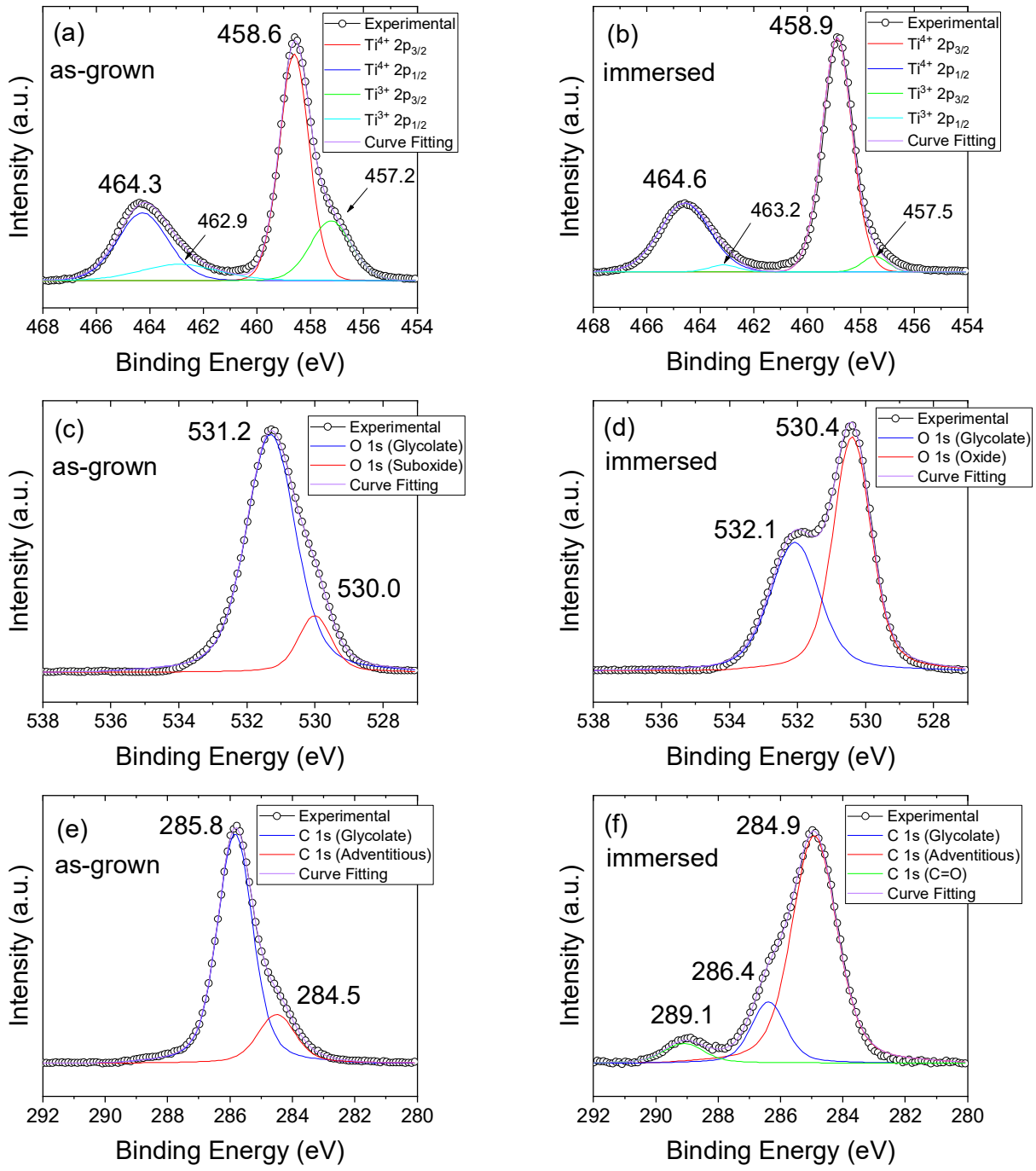

Figure S3. Deconvoluted XPS spectra of (a, b) Ti 2p, (c, d) O 1s, and (e, f) C 1s core electrons of as-grown (110 °C, a, c, f) and water-immersed (b, d, f) titanicone/Si specimens. The numerical values represent the binding energies, measured in electron volts, of deconvoluted spectra. The curve fitting of the doublets of Ti 2p core electrons was performed with two constraints: the intensity ratio (1:2) and the binding energy difference (5.66 eV) of Ti $2p_{1/2}$ and $2p_{3/2}$ [S1].

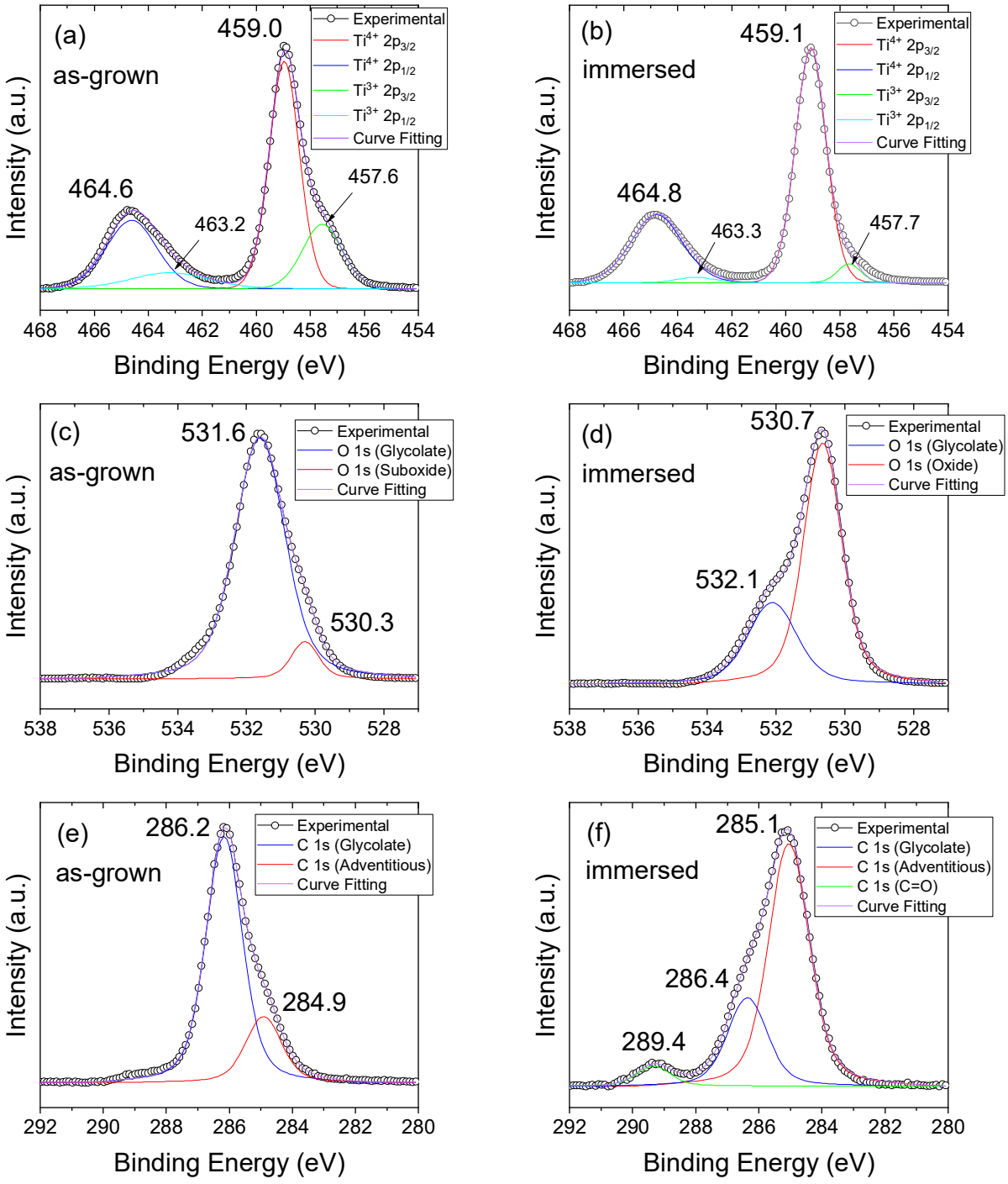

Figure S4. Deconvoluted XPS spectra of (a, b) Ti 2p, (c, d) O 1s, and (e, f) C 1s core electrons of as-grown (80 °C, a, c, f) and water-immersed (b, d, f) titanicone/Si specimens. The numerical values represent the binding energies, measured in electron volts, of deconvoluted spectra. The curve fitting of the doublets of Ti 2p core electrons was performed with two constraints: the intensity ratio (1:2) and the binding energy difference (5.66 eV) of Ti $2p_{1/2}$ and $2p_{3/2}$ [S1].

References

S1. Biesinger, M. C.; Lau, L. W. M.; Gerson, A. R.; Smart, R. S. C. Resolving surface Chemical states in XPS analysis of first row transition metals, oxides and hydroxides: Sc, Ti, V, Cu and Zn. *Appl. Surf. Sci.* **2010**, *257* (3) 887-898.